Crystal Morphology, Microstructure, and Textural Properties of Model Lipid Systems

Yuping Shi, Baomin Liang, and Richard W. Hartel*

University of Wisconsin–Madison, Madison, Wisconsin 53706

ABSTRACT: Mixtures of model lipid systems containing high-melting and low-melting lipid classes were crystallized and microscope images obtained for analysis of crystal morphology and microstructure. Rheological properties of these semisolid systems were tested by use of a texture analyzer. The nature of the high-melting component in a mixture dominated the crystal morphology and, combined with interactions between crystalline and liquid materials, resulted in different microstructures that influenced the rheological properties. In addition to size, shape, and amount (solid fat content) of crystalline material, the crystal packing density, representing how densely the crystalline particles in every level (individual, aggregate, or floc) were arranged, and the nature (or strength) of the link (or bridge) connecting the crystalline particles were important microstructural factors to determine rheological properties. Depending on different crystal packing densities and linking bridges, two different systems were identified in terms of microstructure type—mobile and immobile—in which the relative mobility of microstructural components had different levels. These mobility levels led to different rheological responses.

Paper no. J10975 in *JAOCS 82,* 399–408 (June 2005).

KEY WORDS: Crystallization, crystal network, lipid, microstructure, morphology, rheological properties, texture analysis.

The interactions between TAG solid and liquid phases significantly affect the properties and functionality of semisolid lipid systems. The quality, texture, and shelf stability of lipid-based products, such as butter, margarine, shortenings, chocolate, and compound coatings, are dependent on the lipid crystalline microstructure. Controlling formulation and processing variables in these products to obtain a desired structure will allow us to control their properties.

Natural lipids are complex, containing sometimes up to hundreds of TAG. However, most fats can be described as a combination of a limited number of solid and liquid lipid classes that cover the major TAG components. Thus, studying well-designed lipid classes will allow us to better understand the complex relationships among lipid composition, crystallization parameters, crystalline microstructures, and product textural properties (1–4). Products made with lipid materials of apparently the same physical properties [solid fat content (SFC), m.p., etc.) may result in very different textural properties. The reason for these differences must be in the nature of the crystalline structure formed during processing and storage, but the methods to quantify these different crystalline structures have been limited (5).

Correlations have been developed among the structural attributes, rheological properties, and organoleptic characteristics of various foods (6–8). However, because of the complexity of TAG composition in natural lipids, it is often difficult to predict their physicochemical characteristics. The macroscopic rheological properties of the crystalline network structure are influenced by all levels of structure (the individual TAG, crystalline units, agglomerates, microstructural network, etc.) defined during the formation of the network (9).

It is necessary to consider aspects of both chemical composition (and physical chemistry) and processing conditions to fully understand microstructure and texture/functionality (rheological properties) (9). According to Juriaanse and Heertje (1), hardness of a fat depends on the amount of fat crystals, among other factors, and lipid composition affects the molecular arrangement in crystals, which influences the strength of interactions between crystals. Differences in textural properties between fat-containing products might be attributed to differences in crystalline structure (size, distribution of size, shape, polymorph, surface characteristics, etc.), which are dependent on processing conditions. But differences in crystalline structural characteristics also may be strongly influenced by the interactions between molecules in the crystalline state and the liquid oil in which the crystals are dispersed, leading to different crystalline structural characteristics at different structural levels (crystals, aggregates, and flocs or flocculates). It is generally accepted that a rheological property (e.g., a characteristic modulus) of a fat is a function of SFC and some microstructural factor. Thus, quantification of microstructural characteristics of a semisolid lipid system is the key issue in quantifying this relationship.

A mechanical model of a simple fat network was originally developed by van den Tempel (10), in which the network was composed of straight chains of aggregated fat particles held together by attractive forces. However, it was very difficult to describe the network properties quantitatively owing to the complex and random nature of the structure of the aggregates. Vreeker *et al.* (11) suggested that fat crystal networks had a fractal nature. The fractal dimension was introduced to quantify the relationship between the mass of a cluster and its size (12). In studies on colloidal gels, Shih *et al.* (13) developed a scaling theory in which the gel network was considered to be a

*To whom correspondence should be addressed at Department of Food Science, University of Wisconsin, 1605 Linden Dr., Madison, WI 53706. E-mail: rwhartel@wisc.edu

collection of fractal flocs packed throughout the sample. Elastic constants for two regimes (strong and weak) of linkages between the flocs were defined. By applying the fractal concepts and scaling theory, Marangoni and colleagues developed a model (5,14,15) based on the concept that a viscoelastic lipid system has a fractal attribute. According to this model, fractal dimension was used to represent the microstructural characteristics of the system.

This work investigated the general case of crystalline structure development in different lipid model systems, which were mixtures of different lipid classes with relatively pure TAG composition. The development of crystalline structures was related to the textural attributes of the semisolid lipid systems.

EXPERIMENTAL PROCEDURES

Materials. In this study, three high-melting lipid classes and five low-melting lipid classes with different molecular compositions and melting properties were prepared (Table 1). High-melting lipid classes A, B, and C were tripalmitin (PPP, 98.6% purity) from Sigma Chemical Co. (St. Louis. MO), the solid fraction obtained from fractionation of palm oil, and the solid fraction obtained from two-stage fractionation of cocoa butter, respectively. Based on compositional analysis, they primarily contain trisaturated long-chain (TSLC) TAG, mixed TSLC and disaturated long-chain (DSLC) TAG (PPP, POP, and OOP for 93%), and disaturated long-chain (DSLC) TAG (POP, POS, and SOS for 99.6%), respectively (where P = palmitic acid, O = oleic acid, and S = stearic acid; Table 1). Low-melting lipid classes D, E, F, G, and H were tricaprylin (CCC, >99% purity) from Sigma Chemical Co., purified sunflower oil, purified canola oil, the liquid fraction obtained from multistage fractionation of palm oil, and the liquid fraction obtained from multistage fractionation of lard, respectively. The low-melting fats contained trisaturated short-chain (TSSC) TAG, triunsaturated long-chain (TULC) (18:2) TAG (LLL and LOL for 73%), triunsaturated long-chain (TULC) (18:1) TAG (OOO and OLO for 82%), monosaturated long-chain (MSLC) or diunsaturated long-chain (DULC) TAG (MOO and OOP for 76%), and, mixed MSLC and TULC TAG (OOP, MOO, and OOO for 81%), respectively (where C = caprylic acid, L = linoleic acid, and M = myristic acid; Table 1).

The TAG composition of the lipid classes was analyzed by use of a Hewlett-Packard 5890 GC system (Wilmington, DE) with an Alltech capillary column (Deerfield, IL) (phase: AT-1), based on the method of Lund (16) with modification of the temperature program.

Processing. Lipid mixtures were prepared by mixing each of the three high-melting with each of the five low-melting lipid classes at mass ratios (high- to low-melting) of 4:6, 5:5, and 6:4. A total of 45 different mixtures were studied. The lipid mixtures were melted at 80°C for 1 h to destroy any crystal memory and then cooled to the crystallization temperature in a crystallizer (250-mL glass jacketed beaker) with agitation for isothermal crystallization (no crystallization occurred during cooling). Since the m.p. of the high-melting lipid classes were different, the crystallization temperatures were varied for mixtures of different high-melting classes and different ratios of high-/low-melting classes. After some preliminary trials, crystallization temperatures of 50, 35 or 38, and 21 or 23°C were selected for lipid classes A, B, and C, respectively, with higher crystallization temperatures for the lipid mixtures having a higher ratio of high-/low-melting classes. These temperatures were above the spontaneous nucleation temperatures for these fats, but were still subcooled below the m.p. At these temperatures, crystallization was easily controlled by inducing nucleation with high-intensity agitation (300 rpm) for 30 s to generate nuclei followed by subsequent crystallization with mild agitation (80 rpm) for about 30 min at the same temperature.

A second experimental protocol was followed to document more clearly the morphology of individual fat crystals and their aggregates with polarized light microscopy. In this case, the same induction of nucleation was conducted, followed by static crystallization at the same temperature. In this way, the characteristic morphology of the fat crystals could be observed since little to no agglomeration occurred under the static growth conditions.

After 30 min of crystallization, which gave 90–95% of the maximum yield at the temperature (note that complete equilibrium was not necessary for these studies), slurry samples were

TABLE 1
Chemical Composition (g/100 g identified TAG) and Melting Temperatures (°C) of Lipid Classes in Terms of TAG Groups

Class (major TAG)	TSLC[a]	DSLC[a]	MSLC[a]	TULC[a]	TSSC[a]	MMT[b]
A (TSLC)	98.6	0.0	0.0	0.0	1.4	64.1
B (TSLC-DSLC)	37.8	37.8	17.4	3.3	3.8	56.4
C (DSLC)	0.3	99.6	0.0	0.0	0.1	37.0
D (TSSC)	0.0	0.0	0.0	0.0	100.0	10.3
E (TULC 18:2)	0.1	2.6	21.8	72.8	2.7	–29.3
F (TULC 18:1)	0.9	1.7	12.3	81.7	3.5	–17.0
G (MSLC)	0.3	7.1	76.4	8.9	7.3	17.7
H (MSLC-TULC)	0.5	17.5	64.4	16.9	0.7	20.4

[a]TSLC, trisaturated long-chain; DSLC, disaturated long-chain; MSLC, monosaturated long-chain; TULC, triunsaturated long-chain; TSSC, trisaturated short-chain.
[b]MMT, maximum melting temperature (in °C) from DSC.

taken for microscopic imaging and SFC determination. After the primary crystallization, samples were taken and used to fill NMR test tubes and texture analyzer test cups. The samples were then stored in a constant-temperature environment at 0°C for secondary crystallization at certain periods of time (1, 3, 7, 11, and 21 d). To obtain statistical results, triplicates for each crystallization case were performed.

Characterization of semisolid lipid samples. At the end of primary crystallization, slurry samples of fat crystals were placed on microscope slides and covered with a cover glass. Microstructural images of fat crystals/aggregates/flocs were obtained by use of a Nikon LABOPHOT-2 microscope with polarized light at a magnification of 50×. To observe individual fat crystals at the end of static primary crystallization, a drop of butyl alcohol was used to disperse fat crystals in slurry samples.

The SFC of duplicate samples taken at the end of primary crystallization (still at crystallization temperature) and during storage at 0°C were determined with a Bruker minispec pc-120 NMR system (Bruker, Milton, Ontario, Canada).

A texture analyzer (TA-XT2; Stable Micro Systems, Godalming, Surrey, United Kingdom) was used to characterize the rheological properties of the semisolid fat samples. For compression tests, cylinder-shaped samples cut to have a diameter of 10 mm and a height of 10 mm were compressed a distance of 3.0 mm by a plastic cylindrical probe with a diameter of 12.7 mm and a test speed of 0.1 mm/s. Stress τ (N/cm^2) and natural strain σ (dimensionless) were calculated from the following equations:

$$\tau = \frac{F}{A} \quad [1]$$

$$\sigma = \ln\left(\frac{H}{H - z}\right) \quad [2]$$

where F = compression force (N), A = cross-sectional area of sample (0.785 cm^2), H = sample height (10 mm), and z = distance during compression (mm). For the penetration test, cavity-free samples in a plastic cup with a diameter of 15 mm and a height of 15 mm were penetrated a distance of 6.0 mm by a stainless steel cylindrical probe with a diameter of 3.0 mm at a test speed of 0.5 mm/s. Triplicate tests for each sample were performed at 0°C, and force vs. distance/time was recorded. Stress, the penetration force per unit cross-sectional area of sample, was used to represent the hardness of samples.

Melting profiles of the original lipid classes and semisolid samples during storage were obtained by use of a Pyris 1 DSC system (PerkinElmer, Norwalk, CT) with a temperature scanning program from −50 to 80°C at a heating rate of 5°C/min. The stored sample was directly transferred into the DSC pan and loaded in the machine for scanning.

RESULTS AND DISCUSSION

Crystal morphology and behavior. Crystal slurries were obtained after primary crystallization for the 15 model systems containing 40% high-melting and 60% low-melting lipid classes. Typical microscopic images of these slurries are shown in Figure 1. Although the images were 2-D, they provide somewhat of a stereoscopic view because transmitted light and low magnification were used. These images show fat crystals, crystal aggregates, and flocs and their spatial relationships with the liquid phase in the corresponding systems, from which the different microstructures were formed after secondary crystallization at 0°C. The slurries formed from the static crystallization method were dispersed on the microscope slide to observe the characteristic morphology of the fat crystals. The microscopic images of individual fat crystals and their aggregates for the 15 model lipid systems containing 40% high-melting and 60% low-melting classes are shown in Figure 2.

From Figures 1 and 2, the crystalline lipid was observed as either individual crystals, crystal aggregates, or flocs (flocculates) built with crystal elements (or elementary crystals) depending on the agglomeration level. The crystal units in Figures 1 and 2 had the same characteristics for a certain system since the same induced nucleation method was used. However, the extent of flocculation was different because this was dependent mainly on the dynamic conditions during crystallization.

In Figures 1 and 2, the three columns correspond to high-melting lipid classes A, B, and C, respectively, and the five rows correspond to low-melting lipid classes D, E, F, G, and H, respectively. There are significant differences in morphology between columns (i.e., different high-melting lipid classes), but there is little difference in morphology within a column with the same high-melting lipid class. However, comparison of images in different rows of the same column reveals differences in morphological characteristics such as packing density of crystals/aggregates/flocs, packing orderliness, size of crystal/aggregate/floc, and agglomeration level. A detailed description of each morphology is given in Table 2.

The morphology of crystal elements and their aggregates was mainly dominated by the high-melting lipid class or its TAG saturation level. For systems containing high-melting class A, fat crystals were flake-shaped, and grain-like aggregates were formed. For systems containing high-melting class B, fat crystals were needle-shaped, and typical or regular spherulites were formed. For systems containing high-melting class C, although the elementary crystals were still needle-shaped, irregular spherulites and flocs of these spherulites were built up from the elementary crystals. X-ray analysis (after several days at 0°C) showed that lipid classes A and B were primarily in the β polymorph, whereas lipid class C was in the β' polymorph. Although it is not likely, a polymorphic change might have occurred during this storage period.

In addition, the morphological characteristics of the crystals/aggregates/flocs were affected mainly by the nature of the low-melting lipid class. Of course, the concentration of crystalline materials and processing conditions can also determine the morphological characteristics and the final microstructure; however, this is not the focus of this paper.

The relative strengths of the links between crystal elements in a crystal aggregate or spherulite (intraparticle) and between aggregates or spherulites (interparticle) were an important factor

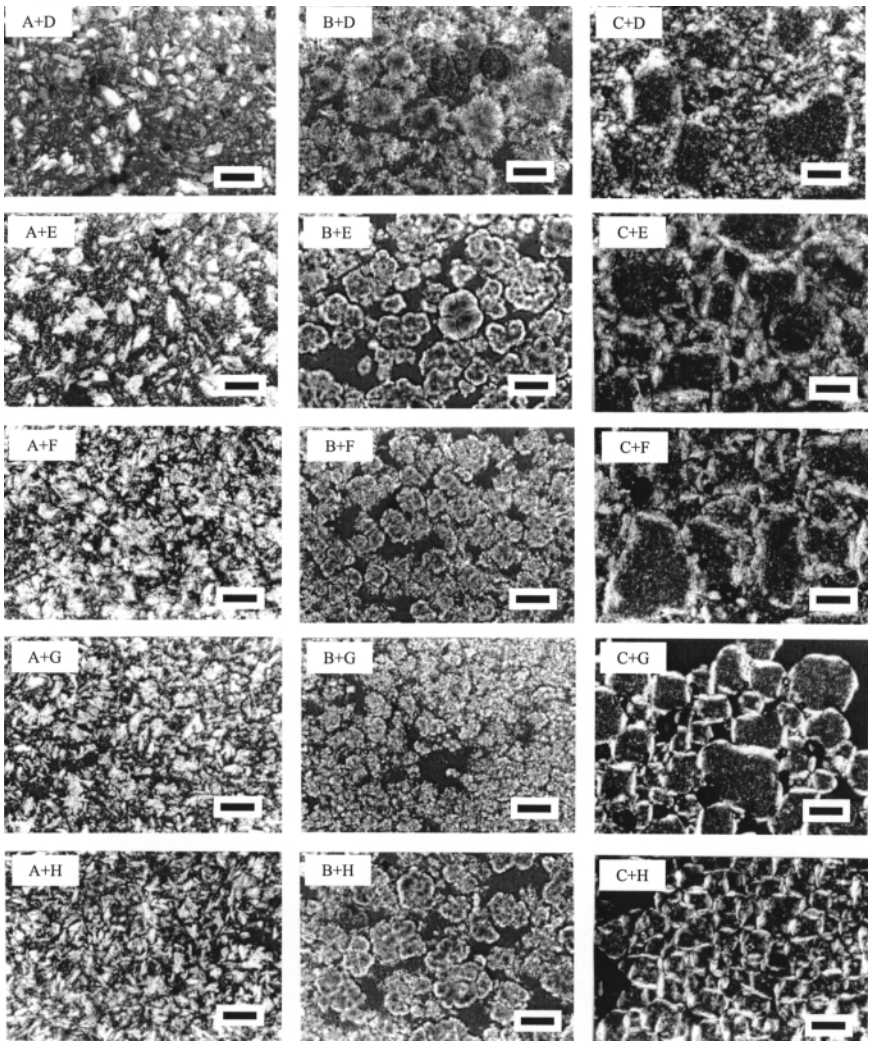

FIG. 1. Polarized light microscopic images of crystals/aggregates/flocs taken at same temperature at the end of primary crystallization in model lipid systems containing 40% high-melting class and 60% low-melting class. See Table 1 for a description of lipid classes A–H. Scale bars represent 100 µm.

affecting microstructure and rheological properties. Since the actual strength of these links could not be quantitatively determined, the relative strength of these links was evaluated based on how orderly and densely packed the elements and particles appeared to be in the microscope images.

Differences in the relative inter- and intraparticle strengths were caused by differences in crystal morphology and the morphological characteristics. For example, densely and orderly packed crystal elements or crystals, as found in systems containing class A or B, most likely had stronger intraparticle links than for the loosely and disorderly packed crystal elements or crystals in systems containing class C. Similarly, for interparticle links, agglomerated lumps or flocculates as in systems of C + G or C + H most likely had stronger interparticle links compared with the isolated and dispersed particles found in systems of B + E or B + F. Thus, it can be considered that, for systems B + E, B + F, A + E, or A + F, the intraparticle link was relatively strong and the interparticle link was relatively weak, and also that for system C + G or C + H, the interparticle link was relatively strong and the intraparticle link was relatively weak.

Interestingly, DSLC TAG (class C) and TULC TAG (class E or F) formed a mixed material that looked and acted somewhat like a gel. This material behaved like a viscous liquid that filled the space between crystals at a higher temperature when it was in the liquid state and became somewhat gel-like (did not flow) to bond crystalline particles together at a lower temperature. Since no structural analysis was performed and the exact nature of this material was uncertain, we call it a "gel-like" material (or LC DS/TU bonding material according to its major TAG components) The existence of this gel-like material between or in the spaces of crystalline particles, as in system C + E or C + F, resulted in a relatively strong interparticle link and a relatively weak intraparticle link.

As discussed in more detail later, the nature and behavior of the continuous materials that mainly consisted of low-melting TAG and connected crystalline particles played a more

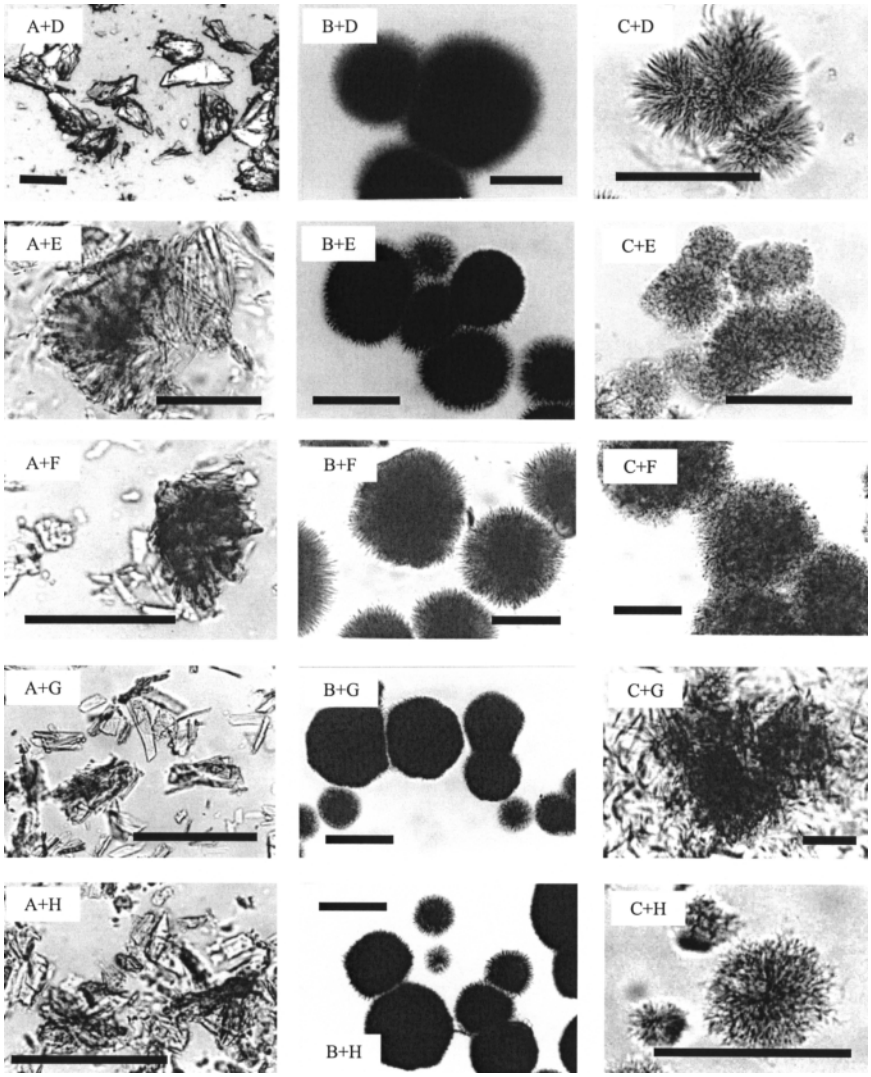

FIG. 2. Images of individually identified crystals/aggregates/flocs showing crystal morphology in model lipid systems containing 40% high-melting class and 60% low-melting class. See Table 1 for a description of lipid classes A–H. Scale bars represent 100 μm.

important role in construction of the network than crystals of high-melting TAG. The relative strengths of intercrystal vs. intra-crystal bonds would affect the microstructure and hence the rheological properties of a system, documented by the large deformation results discussed later.

Melting profiles. When high- and low-melting lipids are crystallized together, numerous interactions might occur among the different TAG. These include interdissolution, dilution (or simple mixing), formation of a solid solution, or other interactions. These interactions may affect the microstructures formed and hence the textural properties of the material. A comparison of the melting profiles of various mixtures with those of the original high- and low-melting lipid components may provide information on these interactions. Furthermore, these interactions may help us understand the nature of the crystalline microstructure formed when different fat systems are crystallized together as well as the resultant hardness of the semisolid fat.

Figure 3 shows typical melting profiles obtained by DSC of several model lipid systems. In general, the maximum melting peaks for the mixtures are shifted to a lower position compared with those for the original high-melting classes. The formation of mixed crystals containing low-melting components reduces the m.p., as observed by a reduction in the peak temperature, or maximum melting temperature (MMT), for the high-melting lipid class (model system C + F is shown as an example in Fig. 3B). A larger MMT drop implied more interaction between high- and low-melting classes in the system. The mean MMT drops (and SD) were 3.57 ± 0.15, 3.69 ± 0.24, and 6.52 ± 0.34°C for systems containing high-melting classes A, B, and C, respectively, indicating there was more interaction between high- and

TABLE 2
Crystal Morphology, Morphological Characteristics and Type of Network Connecting Dispersed Crystalline Particles for Different Model Lipid Systems

High-melting class (major TAG)	A (Trisaturated long-chain)	B (Mixed long-chain)	C (Disaturated long-chain)
Low-melting class (major TAG)			
D (Trisaturated short-chain)	Small, hard, grain-like aggregates with densely packed flake-shaped elements, solid bridge	Typical spherulites with densely and orderly packed needle-shaped elements, solid bridge	Irregular lump of spherulites with tightly and orderly packed needle-shaped elements, solid bridge
E or F (Triunsaturated long-chain)	Large, hard, grain-like aggregates with densely and orderly packed flake-shaped elements, liquid bridge	Typical spherulites with densely and orderly packed needle-shaped elements, liquid bridge	Irregular lump of spherulites with loosely packed needle-shaped elements and filled with gel-like material, gel-like bridge
G (Monosaturated long-chain)	Very small aggregates with loosely and disorderly packed flake-shaped elements, semisolid bridge	Regular spherulites with densely and orderly packed needle-shaped elements, semisolid bridge	Flocculated spherulites with orderly but loosely packed long, filament-shaped elements, semisolid bridge
H (Mixed tri- and di-unsaturated long-chain)	Very small aggregates with loosely and disorderly packed flake-shaped elements, semisolid bridge	Regular spherulites with densely and orderly packed needle-shaped elements, semisolid bridge	Small lump of spherulites with orderly but loosely packed needle-shaped elements, semisolid bridge

low-melting lipids in systems containing class C than in systems containing classes A and B.

The curves for model systems A + D and C + E (Fig. 3A) have major peaks that are only slightly shifted from the peaks of the original high- and low-melting lipid classes. These indicate there was primarily a simple mixing interaction between high- and low-melting components, with dilution of high-melting lipid by the low-melting lipid, although some interdissolution or compound crystal formation of several model lipid systems also may have occurred. This existed in the case where there was a distinct difference in molecular characteristics between high- and low-melting lipids. Model systems containing high-melting class A, low-melting class D, or low-melting class E basically had this character.

Unlike curves for systems A + D and C + E, the melting profiles for systems B + F and C + F (Fig. 3B) had a distinct plateau connecting the shifted peaks from the original high- and low-melting classes. This represents the behavior of significant interdissolution; that is, a significant amount of the high-melting lipid dissolved in the low-melting lipid. This occurred when the molecular characteristics of high- and low-melting lipids were close. Model system B + G also had this behavior.

The melting curves of systems C + H and C + G (Fig. 3C) demonstrate the appearance of a new peak (or group of peaks) and disappearance of the original peaks of the high- and low-melting lipid classes, indicating the formation of a solid solution composed of both high- and low-melting lipid classes. This happened for systems with high- and low-melting lipids having similar TAG molecules. For example, C + H and C + G had partially saturated TAG as the major component. In this case, the solid solution behaved as a distinct entity to give a single thermal event in the DSC profile.

Furthermore, these complex interactions between high- and low-melting lipids might exist simultaneously in a system. For example, interdissolution and formation of solid solution existed simultaneously in model system B + H, since both B and H were relatively complex in terms of TAG composition. Generally speaking, lipid mixtures that have stronger interactions might be expected to lead to stronger links among microstructural components (than mixtures that simply dilute one another) and hence a higher rheological modulus when other factors are the same.

Mechanical properties and network structure. Figure 4 shows typical profiles of stress vs. natural strain as obtained by a compression test at 0°C for model lipid systems containing 40% high-melting class and 60% low-melting class after 1 d of storage. The maximal stress varied from as low as about 1 N/cm^2 (for B + F) to as high as about 260 N/cm^2 (for A + D), indicating that the textural properties were very different from system to system. Comparisons of systems having the same high-melting class but different low-melting class and vice versa revealed that differences in textural properties caused by different low-melting lipids were much larger than those by high-melting lipids.

The microstructure images revealed that the crystal network consisted of crystalline particles, formed *via* primary or secondary crystallization, dispersed in a continuous medium. The crystalline phase forms a network with bridges that might be solid, liquid, semisolid, or "gel-like" as seen in Figure 5 for

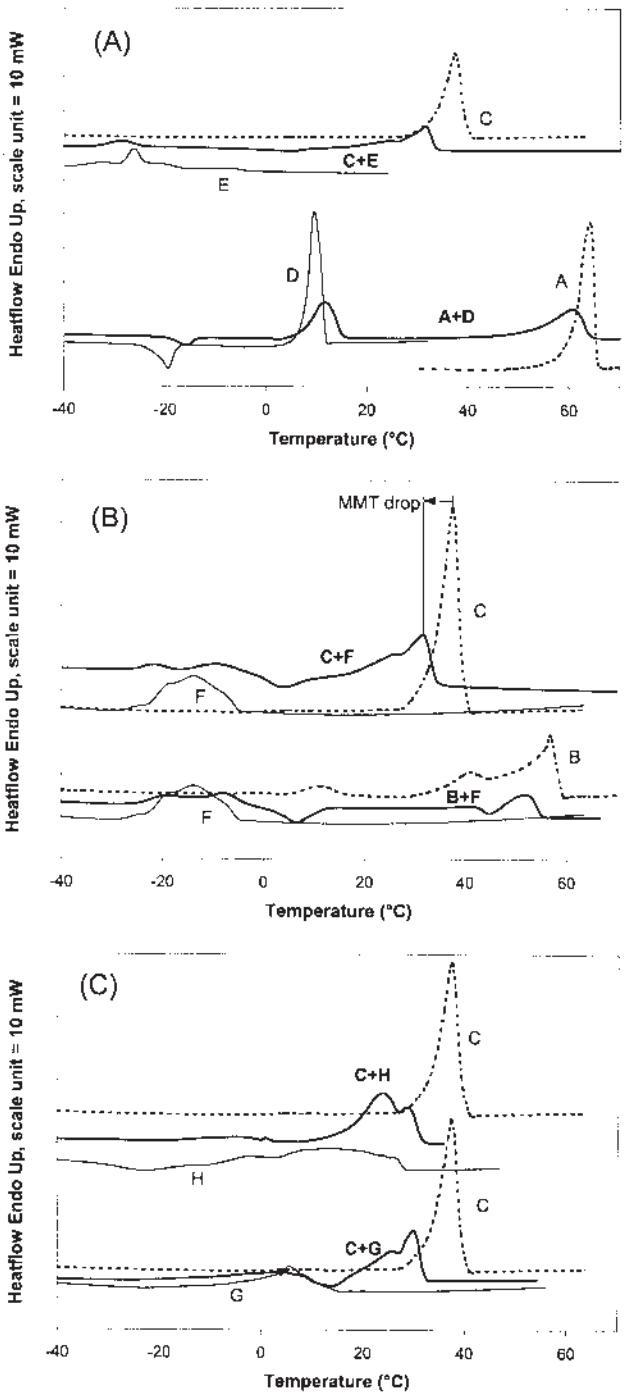

FIG. 3. Typical DSC profiles of model lipid systems showing interactions between high- and low-melting classes. See Table 1 for a description of lipid classes A–H. MMT, maximum melting temperature (°C).

these model systems. The dispersed crystalline particles and/or crystal aggregates/flocs of high-melting lipid are linked by a continuous medium that consists mainly of low-melting lipid. The continuous medium connects the dispersed crystalline particles, and the strength of the bridges influences the crystal network and hence the macroscopic properties of the system.

For a solid bridge, the continuous medium consisted of solidified low-melting TAG since the system was at a low enough temperature for those TAG to solidify. The crystal aggregates or flocs of high-melting TAG were dispersed in the continuous solid material of lower-melting TAG. In this study, the low-melting lipid class D (mainly tricaprylin) was liquid at a higher crystallization temperature but crystallized at the storage temperature of 0°C to form solid bridges. Usually, these solid bridges dramatically increased the strength of the crystal network. Most systems having solid bridges were hard, although some (A + D) were fragile, with very high stress value followed by a breakage feature on stress–strain profiles (Fig. 4).

For a liquid bridge, the continuous medium consisted of liquid oils with TULC TAG as their major components (classes E and F), which remained in a liquid state even at lower temperatures. The crystal aggregates or flocs of high-melting TAG were dispersed in the continuous liquid phase. The liquid bridge provided lubrication and significantly decreased the strength of the crystal network. Systems having a liquid bridge (i.e., mixtures of high-melting classes A or B and low-melting classes E or F) were soft, viscoelastic, and easily deformable with very low and smooth stress values on stress–strain profiles (Fig. 4). The macroscopic rheological properties of these systems were dependent on the amount of liquid per unit surface area of crystalline particles. Thus, in addition to the nature of the low-melting oil, the density, number, size, and shape of crystalline particles affected the macroscopic properties.

Semisolid bridges consisted of both liquid and solid materials, in which fine crystals supported each other to form a continuous crystalline net in the liquid phase. Complex interactions between MSLC TAG (MOO, OOP, etc.) and TULC TAG, which existed mainly in lipid classes G and H, formed solid solutions or compound crystals. The crystal aggregates or flocs of high-melting TAG were dispersed in this continuous semisolid environment. The semisolid bridge enhanced the strength of the crystal network, and systems having semisolid bridges (i.e., high-melting class A, B, or C with a low-melting class G or H) were medium-hard and viscoplastic, having quite high stress values on stress–strain profiles (Fig. 4).

For "gel-like" bridges, "gel-like" or colloidal material was formed by interaction between solid DSLC (or MULC) TAG and liquid TULC TAG to provide a strong link at the interface between liquid and solid. This bridge connected crystal aggregates/flocs and resulted in a continuous crystal network. A substantial amount of liquid oil was immobilized inside the crystal network, increasing its strength, as in mixtures of high-melting class C with low-melting class E or F. For example, when high-melting class C, with lower m.p. than high-melting classes A and B, was mixed with low-melting class E or F, a softer mixture of C and E (or F) would be expected. However, in fact, systems containing high-melting class C and low-melting class E or F were harder, brittle, and less easily deformed, compared with systems containing high-melting class A or B plus a low-melting class E or F. This was indicated by a much higher stress value in Figure 4, because a "gel-like" bridge had been established.

Hardness. Textural, rheological, and mechanical properties of a lipid are affected by many factors. SFC of a system

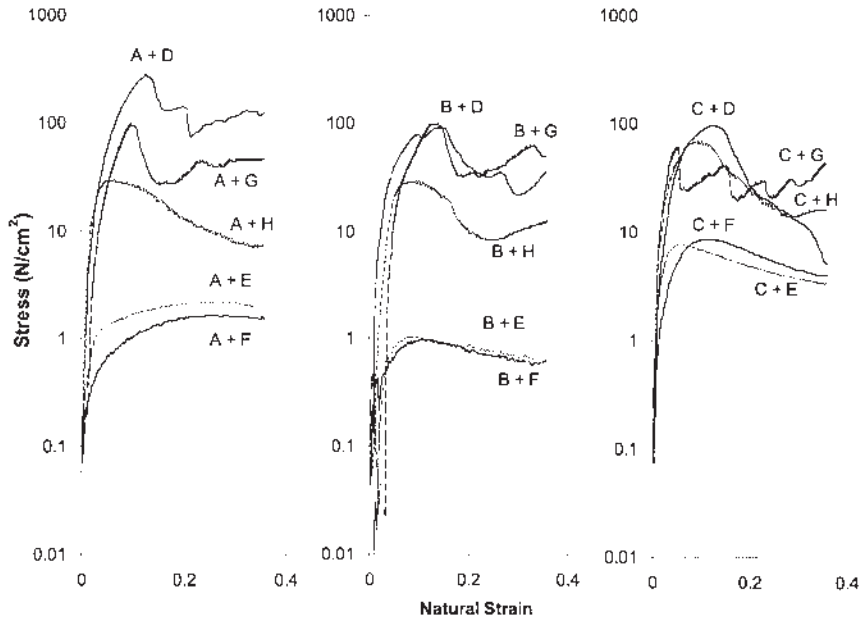

FIG. 4. Profiles of stress vs. natural strain by compression test at 0°C for model lipid systems containing 40% high-melting class and 60% low-melting class after secondary crystallization. See Table 1 for a description of lipid classes A–H.

is generally considered a major factor. SFC depends on the TAG formulation of the mixture, the processing conditions (temperature, etc.), and interactions between solid and liquid lipids. In general, higher SFC leads to higher characteristic moduli. However, crystal morphology and nature, including polymorphic type, shape, hardness of crystal, agglomeration level, crystal size, and how orderly and densely the crystals are packed, also influence macroscopic properties. In addition, the type of bridge connecting the dispersed crystalline particles plays a key role in determining the textural properties. Hardness values, measured as the maximal stress obtained from the penetration test, are given in Table 3 for model systems containing 40% high-melting class and 60% low-melting class after 1 d of storage. Systems with low-melting lipid class D, which led to formation of solid bridges, had the highest hardness, whereas systems containing high-melting class A/B plus low-melting class E/F had the lowest hardness owing to the existence of liquid bridges. However, when high-melting class C was combined with low-melting class E/F, hardness was higher owing to the establishment of a "gel-like" bridge, although C had a lower m.p. and softer character than A/B. Similarly, formation of a solid solution because of stronger interaction between classes C and H caused an increase in hardness compared with those of A/B plus H systems.

Figure 6 shows hardness values plotted against SFC with selected lipid systems representing different typical network structures. Trend lines demonstrate a very good fit to the experimental data, indicating hardness was dependent on SFC basically following a power law model, except for systems (C + E) and (C + F), in which "gel-like" materials were formed. The differences in the textural properties for different systems can be explained by analyzing all affecting factors, in which the

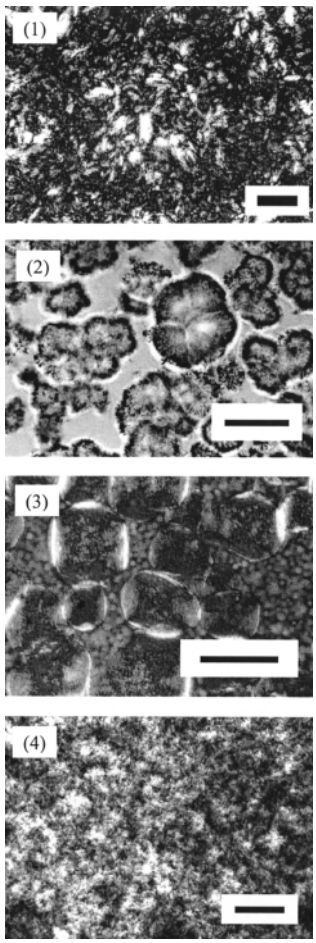

FIG. 5. Networks connecting dispersed crystalline particles: (1) solid bridge, (2) liquid bridge, (3) semisolid bridge, and (4) gel-like bridge; scale bars represent 100 μm.

TABLE 3
Hardness (N/cm^2) by Penetration Test for Model Systems Containing 40% High-Melting Class and 60% Low-Melting Class After 1 d of Storage at 0°C

High-melting class + low-melting class (major TAG)	A (TSLC)[a]	B (TSLC-DSLC)[a]	C (DSLC)[a]
D (TSSC)[a]	$2.78 \times 10^3 \pm 102$ (solid)[b]	446 ± 34 (solid)[b]	188 ± 95 (solid)[b]
E (TULC 18:2)[a]	27.3 ± 1.1 (liquid)[b]	7.6 ± 0.6 (liquid)[b]	53.4 ± 12.6 (gel-like)[b]
F (TULC 18:1)[a]	21.4 ± 1.3 (liquid)[b]	5.8 ± 0.1 (liquid)[b]	69.4 ± 7.1 (gel-like)[b]
G (MSLC)[a]	421 ± 12 (semisolid)[b]	308 ± 5 (semisolid)[b]	300 ± 18 (semisolid)[b]
H (MSLC-TULC)[a]	119 ± 1 (semisolid)[b]	56.1 ± 1.7 (semisolid)[b]	276 ± 11 (semisolid)[b]

[a]For abbreviations see Table 1.
[b]Network (bridge) type.

network (bridge) type can be considered an eventually dominating parameter. For example, systems of A/B/C plus D had higher stress and hardness because a solid bridge was formed; in particular, for system (A + D), dense and hard crystals of TSLC TAG led to a maximum hardness. Systems with liquid bridges, such as A/B + E/F, had very low stress or hardness. However, systems C + E or F had higher hardness than systems A or B + E or F owing to formation of a "gel-like" bridge, even if the m.p. of C was lower than those of A and B.

The concept of microstructure should include information about the state, amount, shape, size, spatial relation, and interaction of all the components (solids, liquids, etc.) in a system. For lipid systems, SFC, polymorphic type, morphology of crystalline materials, type of bridges connecting crystalline particles, and the relative strength of intracrystalline bonds and intercrystalline links are microstructural characteristics that affect macroscopic properties. In this case, lipid microstructure may be loosely classified into two different types (mobile or immobile) based on the relative strength of links within the crystalline particles and between adjacent crystalline particles. This is the relative mobility of microstructural components.

For a mobile-type microstructure, the crystalline particles had a higher packing density and were dispersed in a continuous liquid oil phase or a semisolid environment so that there

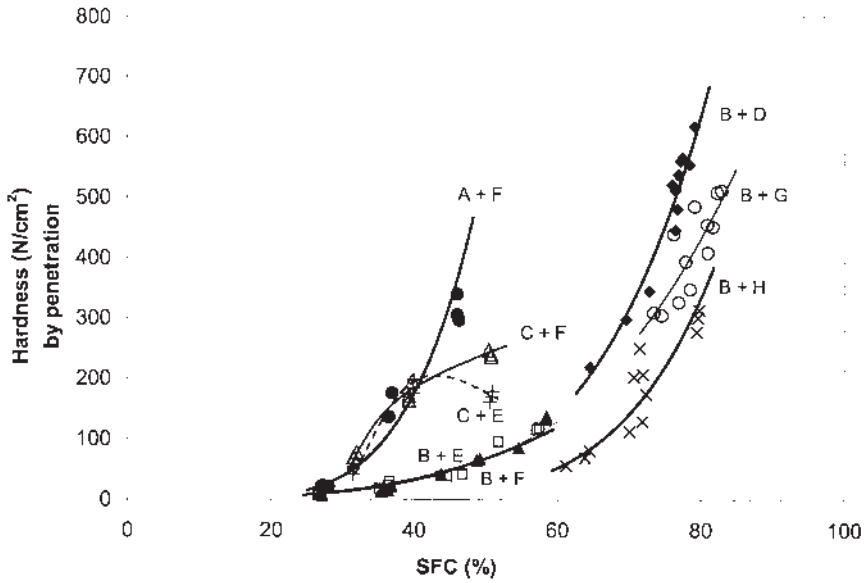

FIG. 6. Relationships between solid fat content (SFC) and hardness obtained by penetration test at 0°C after secondary crystallization for model lipid systems having different ratios of high-/low-melting classes and SFC values. See Table 1 for a description of lipid classes A–H. Lines reflect a power-law fitting except systems C + F and C + E.

was a stronger link within the crystalline particles than between crystalline particles, and relative movement of microstructural components occurred easily. Systems with a network of liquid and semisolid bridges basically belonged to this type. The amount of liquid TAG distributed to the unit surface area of crystalline particles was a key factor dominating the macroscopic rheological properties of the system. If this value is high, the liquid-filled space will be large, the resistance to the relative movement will be decreased, and the relative displacement of microstructural components will be easy. Thus, the system will be soft and easily deformable. For a system with a certain formulation, its SFC and liquid amount are relatively fixed. Therefore, size, shape, and packing density of the crystalline particles will determine the amount of liquid TAG distributed to a unit surface area of crystalline particles and hence the macroscopic properties.

For an immobile-type microstructure, as in systems with a network of solid and "gel-like" bridges, there was a stronger link between crystalline particles than that within a crystalline particle. This made the relative displacement of microstructural components impossible and hence gave relatively higher hardness.

ACKNOWLEDGMENT

The authors gratefully acknowledge the USDA for financial support *via* the National Research Initiative Competitive Grants Program.

REFERENCES

1. Juriaanse, A.C., and I. Heertje, Microstructure of Shortenings, Margarine and Butter—A Review, *Food Microstruct. 7*:181–188 (1988).
2. Heertje, I., Microstructural Studies in Fat Research, *Food Struct. 12*:77–94 (1993).
3. Shukla, A., and S.S.H. Rizvi, Relationship Among Chemical Composition, Microstructure and Rheological Properties of Butter, *Milchwissenschaft 51 (3)*:144–148 (1996).
4. Marangoni, A.G., and D. Rousseau, Is Plastic Fat Rheology Governed by the Fractal Nature of the Fat Crystal Network? *J. Am. Oil Chem. Soc. 73*:991–994 (1996).
5. Marangoni, A.G., and R.W. Hartel, Visualization and Structural Analysis of Fat Crystal Networks, *Food Technol. 52(9):*46–51 (1998).
6. Kokini, J.L., Fluid and Semi-solid Food Texture and Texture–Taste Interactions, *Ibid. 39(11)*:86–92 (1985).
7. Kokini, J.L., and E.L. Cussler, The Psychophysics of Fluid Food Texture, in *Food Texture*: *Instrumental and Sensory Measurement*, edited by H.R. Moskowitz, Marcel Dekker, New York, 1987, pp. 97–127.
8. Kokini, J.L., and E.L. Cussler, Predicting the Texture of Liquid and Semi-solid Foods, *J. Food Sci. 48*:1221–1225 (1983).
9. Narine, S.S., and A.G. Marangoni, Fractal Nature of Fat Crystal Networks, *Phys. Rev. E 59*:1908–1920 (1999).
10. van den Tempel, Mechanical Properties of Plastic Disperse Systems at Very Small Deformations, *J. Colloid Sci. 16*:284–296 (1961).
11. Vreeker, R., L.L. Hoekstra, D.C. den Boer, and W.G.M. Agterof, The Fractal Nature of Fat Crystal Networks, *Colloids Surf. 65*:185–189 (1992).
12. Meakin, P., Fractal Aggregates, *Adv. Colloid Interface Sci. 28*:249–331 (1988).
13. Shih, W.H., W.Y. Shih, S.I. Kim, J. Liu, and I.A. Aksay, Scaling Behavior of the Elastic Properties of Colloidal Gels, *Phys. Rev. A 42*:4772–4779 (1990).
14. Marangoni, A.G., The Nature of Fractality in Fat Crystal Networks, *Trends Food Sci. Technol. 13*:37–47 (2002).
15. Narine, S.S., and A.G. Marangoni, Mechanical and Structural Model of Fractal Network of Fat Crystals at Low Deformations, *Phys. Rev. E 60*:6991–7000 (1999).
16. Lund, P., Analysis of Butterfat Triglycerides by Capillary Gas Chromatography, *Milchwissenschaft 43*:159–161 (1988).

[Received October 26, 2004; accepted May 19, 2005]